Static and Dynamic ^{68}Ga-FAPI PET/CT for the Detection of Malignant Transformation of Intraductal Papillary Mucinous Neoplasia of the Pancreas

Matthias Lang[1], Anna-Maria Spektor[2], Thomas Hielscher[3], Jorge Hoppner[2], Frederik M. Glatting[2,4,5], Felix Bicu[2], Thilo Hackert[1], Ulrike Heger[1], Thomas Pausch[1], Ewgenija Gutjahr[6], Hendrik Rathke[2,7], Frederik L. Giesel[2,8], Clemens Kratochwil[2], Christine Tjaden[1], Uwe Haberkorn[2,9,10], and Manuel Röhrich[2]

[1]Department of General, Visceral, and Transplantation Surgery, University Hospital Heidelberg, Heidelberg, Germany; [2]Department of Nuclear Medicine, University Hospital Heidelberg, Heidelberg, Germany; [3]Department of Biostatistics, German Cancer Research Center, Heidelberg, Germany; [4]Clinical Cooperation Unit Molecular and Radiation Oncology, German Cancer Research Center (DKFZ), Heidelberg, Germany; [5]Department of Radiation Oncology, University Hospital Heidelberg, Heidelberg, Germany; [6]Department of Pathology, University Hospital Heidelberg, Heidelberg, Germany; [7]Department of Nuclear Medicine, The Inselspital, Bern University Hospital, University of Bern, Bern, Switzerland; [8]Department of Nuclear Medicine, University Hospital Düsseldorf, Düsseldorf, Germany; [9]Translational Lung Research Center Heidelberg (TLRC), Member of the German Center for Lung Research DZL, Heidelberg, Germany; and [10]Clinical Cooperation Unit Nuclear Medicine, German Cancer Research Center (DKFZ), Heidelberg, Germany

Pancreatic ductal adenocarcinoma (PDAC) may arise from intraductal papillary mucinous neoplasms (IPMN) with malignant transformation, but a significant portion of IPMN remains to show benign behavior. Therefore, it is important to differentiate between benign IPMN and IPMN lesions undergoing malignant transformation. However, nonoperative differentiation by ultrasound, CT, MRI, and carbohydrate antigen 19-9 (CA19-9) is still unsatisfactory. Here, we assessed the clinical feasibility of additional assessment of malignancy by PET using ^{68}Ga-labeled fibroblast activation protein inhibitors (^{68}Ga-FAPI PET) in 25 patients with MRI- or CT-proven cystic pancreatic lesions. **Methods:** Twenty-five patients with cystic pancreatic lesions who were followed up in the European Pancreas Center of Heidelberg University hospital and who were led to surgical resection or fine-needle aspiration due to suspicious clinical, laboratory chemistry, or radiologic findings were examined by static (all patients) and dynamic (20 patients) ^{68}Ga-FAPI PET. Cystic pancreatic lesions were delineated and SUV_{max} and SUV_{mean} were determined. Time–activity curves and dynamic parameters (time to peak, K_1, k_2, K3, k_4) were extracted from dynamic PET data. Receiver-operating curves of static and dynamic PET parameters were calculated. **Results:** Eleven of the patients had menacing IPMN (high-grade IPMN with [6 cases] or without [5 cases] progression into PDAC) and 11 low-grade IPMN; 3 patients had other benign entities. Menacing IMPN showed significantly elevated ^{68}Ga-FAPI uptake compared with low-grade IPMN and other benign cystic lesions. In dynamic imaging, menacing IPMN showed increasing time–activity curves followed by slow decrease afterward; time–activity curves of low-grade IPMN showed an immediate peak followed by rapid decrease for about 10 min and slower decrease for the rest of the time. Receiver-operating curves showed high sensitivity and specificity (area under the curve greater than 80%) of static and dynamic PET parameters for the differentiation of IPMN subtypes. **Conclusion:** ^{68}Ga-FAPI PET is a helpful new tool for the differentiation of menacing and low-grade IPMN and shows the potential to avoid unnecessary surgery for nonmalignant pancreatic IPMN.

Key Words: fibroblast activation protein; FAPI; PET; dynamic PET; cancer; PDAC; IPMN

J Nucl Med 2023; 64:244–251
DOI: 10.2967/jnumed.122.264361

The pancreatic ductal adenocarcinoma (PDAC) belongs to the most lethal cancers, with a poor 5-y survival rate of less than 10% despite surgical resection, radiotherapy, and chemotherapy (*1*). Intraductal papillary mucinous neoplasms (IPMN) with high-grade dysplasia (hg-IPMN) are precursors for malignant transformation into PDAC (*2*). Therefore, resection of hg-IPMN before the development of invasive PDAC is mandatory (*3,4*). hg-IPMN with and without development into PDAC are grouped together in this article as menacing IPMN (men-IPMN). In contrast, IPMN with low-grade dysplasia (lg-IPMN) are regarded as benign lesions that should be controlled regularly but not resected (*3,4*). Regarding the significant risk of complications in pancreatic surgery (morbidity rates of 35%–50% and mortality rates up to 1% (*5,6*)), the selective resection of men-IPMN is an important goal.

Currently, evaluation of IPMN regarding malignant potential is controversial and mostly based on the Fukuoka consensus criteria of 2017 or the European guidelines for pancreatic cystic neoplasms. Both rely on multiple clinical and morphologic parameters (*3,4*). However, several publications have shown the shortcomings of these guidelines due to their limited specificity and sensitivity (*7–9*). Recent studies revealed that only 35% of IPMN were resected in a timely fashion (*10*). Therefore, the decision for surgical treatment remains challenging, and clinical tools to distinguish between lg-IPMN and men-IPMN are urgently needed.

PET using ^{68}Ga-labeled fibroblast activation protein inhibitors combined with CT (^{68}Ga-FAPI PET/CT) has shown excellent

Received May 2, 2022; revision accepted Jul. 16, 2022.
For correspondence or reprints, contact Manuel Röhrich (manuel.roehrich@med.uni-heidelberg.de).
Published online Jul. 29, 2022.

imaging properties and high clinical potential for PDAC. The intense FAPI tracer accumulation in PDAC is based on the strong stromal portion of PDAC including fibroblast activation protein (FAP)–positive cancer-associated fibroblasts (*11*). We hypothesized that FAP-positive stroma could be a common feature of PDAC and men-IPMN, but not of lg-IPMN, as the desmoplastic stromal reaction is a prominent hallmark of malignancy but not of benign lesions (*12*). Here, we retrospectively analyzed preoperative static and dynamic ^{68}Ga-FAPI PET data of 25 patients with suspected IPMN and compared imaging features with histologic diagnoses to evaluate the potential value of ^{68}Ga-FAPI PET for the differentiation of lg- and men-IPMN.

MATERIALS AND METHODS

Patient Characteristics

Patients were selected for ^{68}Ga-FAPI PET according to the following criteria: age, 18 y or older; MRI- or CT-proven pancreatic cyst leading to the clinical diagnosis of IPMN; absolute or relative indication for surgery; and sufficient compliance for and consent to the ^{68}Ga-FAPI PET procedure. All patients conforming to these selection criteria who presented in the European Pancreas Center Heidelberg during the examination period (June 2020 to December 2021) were included in our analysis. Twenty-five patients (mean age, 63.8 y; maximum age, 83 y; minimum age, 38 y; 13 men) with contrast-enhanced MRI- (24 patients) or CT- (2 patients) proven cystic pancreatic lesions planned for surgery underwent ^{68}Ga-FAPI PET imaging. All patients were referred by their treating physicians to exclude metastatic disease. Additionally, in 8 patients an endoscopic ultrasound (EUS)–guided fine-needle aspiration (FNA) cytology was obtained. No malignant results were found. Clinical diagnosis of IPMN was based on the identification of a cystic lesion larger than 10 mm, related to the pancreatic main duct, or a main duct dilatation of more than 5 mm without signs of chronic pancreatitis using MRI or CT. All patients had a relative or absolute indication for pancreatic surgery according to recent European guidelines (*4*). In 7 patients the diameter of the pancreatic main duct exceeded 10 mm, in 1 patient diameter was more than 5 mm, and 1 patient presented with jaundice. Four patients showed an elevated carbohydrate antigen 19-9 (CA 19-9) level and 9 a branch duct dilatation greater than 40 mm; in 1 patient an enhancing mural nodule less than 5 mm was detected. One female presented symptomatic with recurrent IPMN-related acute pancreatitis. Tumor marker

TABLE 1
Clinical Characteristics and Histologic Diagnoses of 25 Patients with Suspected IPMN and ^{68}Ga-FAPI-74 PET/CT

Patient	Sex	Age (y)	Cyst size (mm)	IPMN type	Additional information	Surgery/histology	Histologic diagnosis
1	M	52	29	BD		Whipple	lg-IPMN
2	F	52	57	BD		Excision	lg-IPMN
3	M	76	40	BD		Cytology	lg-IPMN
4	F	42	30	BD		Whipple	lg-IPMN
5	M	71	60	BD		Whipple	lg-IPMN
6	F	67	44	BD		Distal pancreatectomy	lg-IPMN
7	M	56	18*	MD	Mural nodule	Enucleation	hg-IPMN
8	M	79	10*	MD		Whipple	hg-IPMN
9	M	53	20*	MD		Distal pancreatectomy	PDAC
10	F	64	11*	MD		Whipple	PDAC
11	M	68	32	BD	MD with dliatation to 4.8 mm, jaundice	Whipple	PDAC
12	F	44	10*	Mixed type		Distal pancreatectomy	hg-IPMN
13	F	57	50*	MD		Pancreatectomy	PDAC
14	M	78	90	Mixed type	Solid components	Therapy refused	None
15	F	74	25	BD	Size progressing	Distal pancreatectomy	hg-IPMN
16	F	80	42	BD		Distal pancreatectomy	PDAC
17	F	83	45	BD		Distal pancreatectomy	PDAC
18	M	63	30	BD		Cytology (nonconclusive)	None
19	M	77	60	BD		Cytology	None
20	F	64	30	BD		Cytology (nonconclusive)	None
21	F	57	23	BD	Size progressing	None	None
22	M	74	10	BD		None	None
23	F	54	38			Cytology	SCN
24	F	38	38			Distal pancreatectomy	SCN
25	M	62	21			Distal pancreatectomy	PanIN

*Main duct diameter.
BD = branch duct; MD = main duct; SCN = serous cystic neoplasia; PanIN = pancreatic intraepithelial neoplasia.

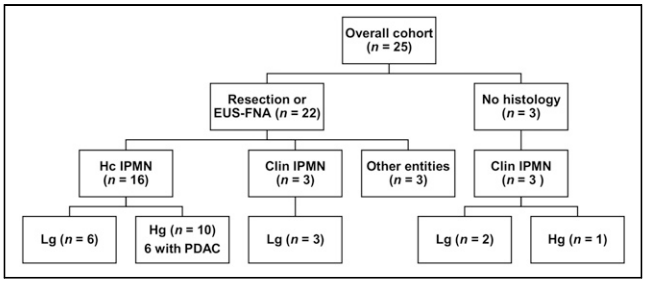

FIGURE 1. Histologic diagnoses and clinical classification of 25 patients with suspected IPMN who underwent ^{68}Ga-FAPI PET/CT. clin IPMN = clinical IPMN; EUS-FNA = endoscopic ultrasound–guided fine-needle aspiration; hc IPMN = histologically confirmed IPMN; hg = high grade; lg = low grade; PDAC = pancreatic ductal adenocarcinoma.

carcinoembryonic antigen was moderately elevated in 1 individual (3.4 μg/L, upper limit of normal [ULN] 2.5), who had a highly elevated CA 19-9 (476 U/mL, ULN 37) too. The following absolute or relative criteria for resection according to the European guidelines (*4*) were not observed: EUS-guided malignant cytology/histology, growth rate of branch duct IPMN (BD-IPMN) greater than 5 mm per year, and new onset of diabetes mellitus. Table 1 provides a detailed patient-wise overview of clinical characteristics and histologic diagnoses.

^{68}Ga-FAPI PET/CT Imaging

Synthesis and labeling of ^{68}Ga-FAPI-74 were conducted as previously described (*13–15*). For PET imaging, a Biograph mCT Flow scanner (Siemens) was used, according to previously published protocols (*16*). In short, after a low-dose CT without contrast, 3-dimensional PET scans were acquired (matrix, 200 × 200), reconstructions performed, and emission data corrected for attenuation. For all patients, static PET scans were acquired at 60 min after administration of 180–329 MBq of ^{68}Ga-labeled FAPI-74. To characterize early ^{68}Ga-FAPI-74 uptake kinetics, additional dynamic PET scanning was performed in 20 patients as previously described (*16*).

Image Evaluation

For static PET scans, SUV_{max} and SUV_{mean} of cystic pancreatic lesions and healthy organs were analyzed using a volume of interest (VOI) technique. VOIs were defined by an automatic isocontour with a cutoff at 50% of SUV_{max}. For dynamic PET imaging analysis, VOIs of cystic lesions and aortal blood were drawn and applied to the entire dynamic dataset. Time–activity curves of ^{68}Ga-FAPI-74 uptake were obtained, and time to peak (TTP) values (minutes from the beginning of the dynamic acquisition to the SUV_{max} of the lesion) were derived from these. Kinetic modeling using a 2-compartment model was performed to generate K_1 and k_2 values. Dynamic data analysis was performed using PMOD software (PMOD Technologies Ltd.).

Statistical Analysis

Receiver-operating curve (ROC) analysis was used to assess discriminative ability of PET parameters. Area under the ROC curve with corresponding 95% CI using Delong's method (*17*) was computed using R package pROC (*18*).

RESULTS

Histologic Results and Surgical Management of the Patients

Twenty-two of 25 patients examined by ^{68}Ga-FAPI PET/CT underwent resection or EUS-FNA. Six of these 22 patients had a histologically confirmed (hc) lg-IPMN. Ten of 22 patients had a hc men-IPMN (6 of them with transition into PDAC). In 3 of 22 patients, EUS-guided fluid aspiration strongly indicated a mucinous lesion without signs of malignancy; thus, we considered these cases as clinical lg-IPMN. Three of 22 patient had a histologic confirmation of entities other than IPMN (2 serous cystic neoplasia, 1 pancreatic intraepithelial neoplasia). Three of 25 patients had no histologic confirmation. Because of radiologic appearance and clinical course, 2 patients were considered as clinical lg-IPMN and 1 as clinical hg-IPMN (Fig. 1). Of the 10 patients with hc men-IPMN, 5 underwent distal pancreatectomy, 3 pancreatoduodenectomy, 1 complete pancreatectomy, and 1 enucleation. Of 6 patients with hc lg-IPMN, 2 underwent pancreaticoduodenectomy, 1 distal pancreatectomy, and 1 enucleation. Two patients underwent EUS-FNA only and are still under surveillance without any complications. As ^{68}Ga-FAPI-74 PET imaging did not reveal any metastatic diseases, it did not influence the surgical management of the patients analyzed.

^{68}Ga-FAPI-74 Biodistribution and Uptake of Men-IPMN and Low-Grade IPMN

On the basis of static PET images acquired at 1 h after injection, normal tissues including the healthy part of the pancreas all showed low SUV_{max} and SUV_{mean} resulting in low background signal for the analysis of pathologies (Fig. 2A). Clinical and hc men-IPMN showed markedly higher ^{68}Ga-FAPI-74 uptake than clinical and hc lg-IPMN and other pathologies (Figs. 3A and 3B). Of note, hg-IPMN, which had already undergone malignant progression into PDAC, showed higher SUV_{max} and SUV_{mean} than those without (Supplemental Fig. 1; supplemental materials are available at http://jnm.snmjournals.org). Grouped according to surgical management, ^{68}Ga-FAPI-74 uptake of lesions with an indication for surgery (hc and clinical men-IPMN) was significantly higher than that of lesions without (hc and clinical lg-IPMN and other pathologies) (Figs. 3C and 3D).

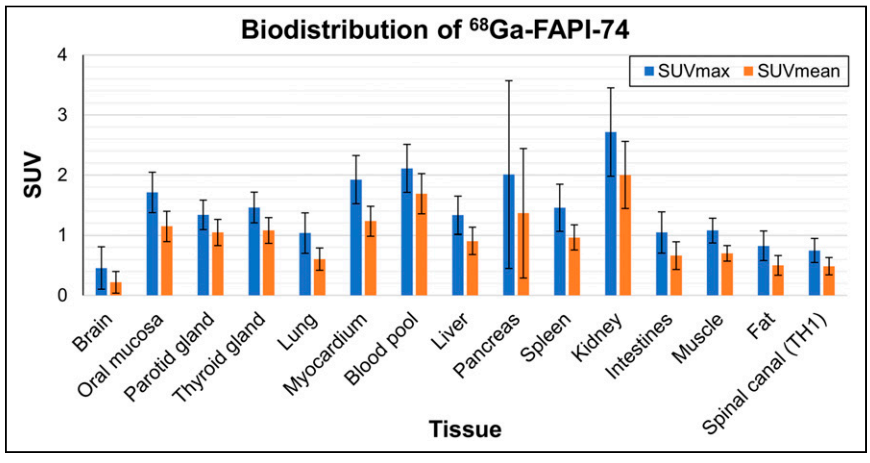

FIGURE 2. Biodistribution analysis (SUV_{max} and SUV_{mean} ± SD) of 25 patients with suspected IPMN based on static PET imaging at 1 h after injection of ^{68}Ga-labeled FAPI-74.

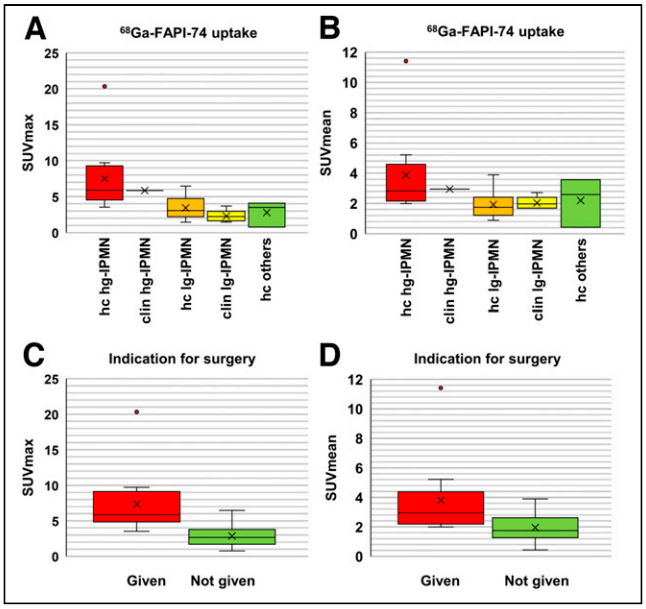

FIGURE 3. (A and B) Boxplots of SUV_{max} (A) and SUV_{mean} (B) of different types of cystic pancreatic lesions. (C and D) Boxplots of SUV_{max} (C) and SUV_{mean} (D) sorted by given or not given indication for surgery. Boxes represent the interquartile range (IQR) and whiskers the range of 1.5 IQR; horizontal line within box indicates the median and cross the mean. Data outliers are shown separately within graph. clin hg-IPMN = clinical high-grade IPMN; clin lg-IPMN = clinical low-grade IPMN; hc hg-IPMN = histologically confirmed high-grade IPMN; hc lg-IPMN = histologically confirmed low-grade IPMN; hc others = histologically confirmed other entities.

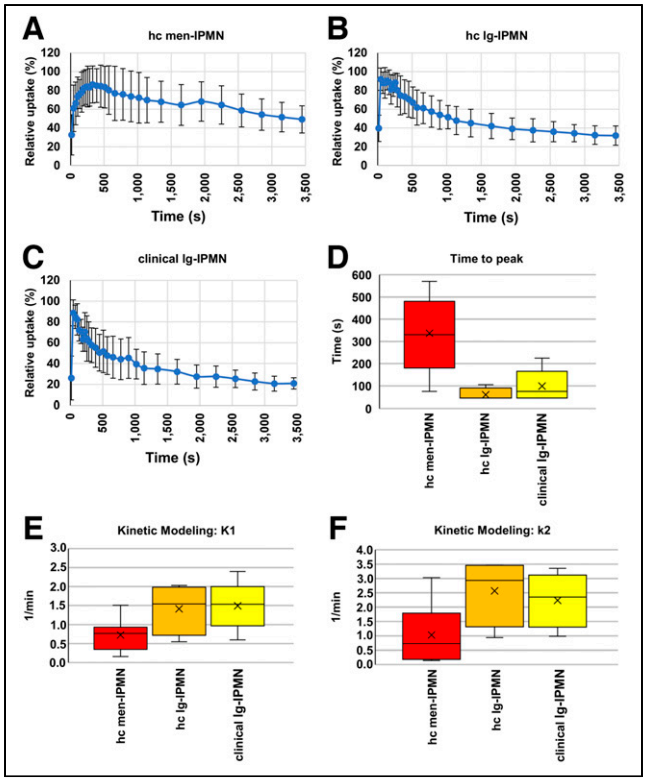

FIGURE 4. (A–C) Time–activity curves displaying averaged ^{68}Ga-FAPI-74 uptake (relative to peak) kinetics of histologically confirmed menacing IPMN (hc men-IPMN) (A), histologically confirmed low-grade IPMN (hc lg-IPMN) (B), and clinical low-grade IPMN (clin lg-IPMN) (C). (D) Box plot displaying time to peak values of histologically confirmed menacing IPMN, histologically confirmed low-grade IPMN, and clinical low-grade IPMN as measured by dynamic ^{68}Ga-FAPI-74 PET imaging. (E and F) Box plots displaying K_1 (E) and k_2 (F) values of histologically confirmed menacing IPMN, histologically confirmed low grade IPMN, and clinical low-grade IPMN as calculated by kinetic modeling of dynamic ^{68}Ga-FAPI-74 PET imaging data. Boxes represent the interquartile range (IQR) and whiskers the range of 1.5 IQR; horizontal line within box indicates the median and cross the mean. Data outliers are shown separately within graph.

Dynamic Imaging

Dynamic ^{68}Ga-FAPI-74 PET was performed in 20 patients (9 with hc men-IPMN, 4 with hc lg-IPMN, 5 with clinical lg-IPMN and 2 with other pathologies [not evaluated]). Time–activity curves of hc men-IPMN differed markedly from those of hc and clinical lg-IPMN. Whereas hc men-IPMN showed an increasing time–activity curve for about 6 min and slowly decreasing time–activity curves afterward, hc and clinical lg-IPMN showed an immediate peak followed by rapid decrease for about 10 min and slower decrease for the rest of the time (Figs. 4A–4C). The delayed increase and prolonged washout of the tracer in men-IPMN compared with lg-IPMN are also reflected by increased TTP (Fig. 4D). Kinetic modeling using a 2-tissue-compartment model revealed decreased K_1 and k_2 values (Figs. 4E and 4F) as well as decreased K3 and k_4 values (Supplemental Fig. 2) of men-IPMN compared with lg-IPMN.

Sensitivity and Specificity

Figure 5 shows ROCs displaying the sensitivity and specificity of SUV_{max}, SUV_{mean}, and TTP for the distinction between hc lg-IPMN and hc men-IPMN (Fig. 5A) and between entities requiring surgery or not (Fig. 5B). For all parameters, the area under the curve (AUC) was greater than 80%, suggesting a high discriminatory power of static and dynamic ^{68}Ga-FAPI PET for both distinctions, whereas TTP showed slightly higher AUC values than static parameters for both distinctions (for men-IPMN vs. lg-IPMN: 97.2% vs. 86.7% [SUV_{max}] and 88.3% [SUV_{mean}], for indication for surgery 92.6% vs. 91.6% [SUV_{max}] and 81.8% [SUV_{mean}]). Table 2 provides thresholds and specificities at fixed sensitivities of 90% and 80%, including 95% CIs for SUV_{max}, SUV_{mean}, and TTP with respect to the discrimination of hc men-IPMN and hc lg-IPMN and given or not given indication for surgery.

Case Vignette

In Figure 6, 3 representative cases are highlighted. The patient with PDAC based on an IPMN is a 68-y-old male, who presented in our department with slight jaundice and brown urine. A weight loss of 6 kg in 3 wk had occurred. Otherwise, the patient was completely asymptomatic. Laboratory results revealed a bilirubin of 8.1 mg/dL (ULN 1.0) and a CA 19-9 of 341.9 U/mL (ULN 37). In contrast-enhanced (ce) MRI, a double duct sign and several cystic lesions of the pancreatic head were apparent. There was no visible solid mass in the pancreas. A malignant transformation of a mixed-type IPMN was diagnosed. To exclude extrapancreatic manifestation, a ^{68}Ga-FAPI PET/CT image was obtained. The pancreatic head showed intense ^{68}Ga-FAPI uptake, indicating pancreatic tumor. As no metastatic lesions were apparent, a Whipple procedure was performed. Histologically an adenocarcinoma of the pancreatic head (35 mm), based on a mixed-type IPMN with high-grade dysplasia, was confirmed (pT2, pN2 [19/26], L1, V1, Pn1, G3, R0, CRM+). For the patient with hg-IPMN without progression into PDAC, a woman aged 44 y, randomly determined elevated pancreatic enzymes led to an MRI examination. The examination showed dilation of the main pancreatic duct by 10 mm

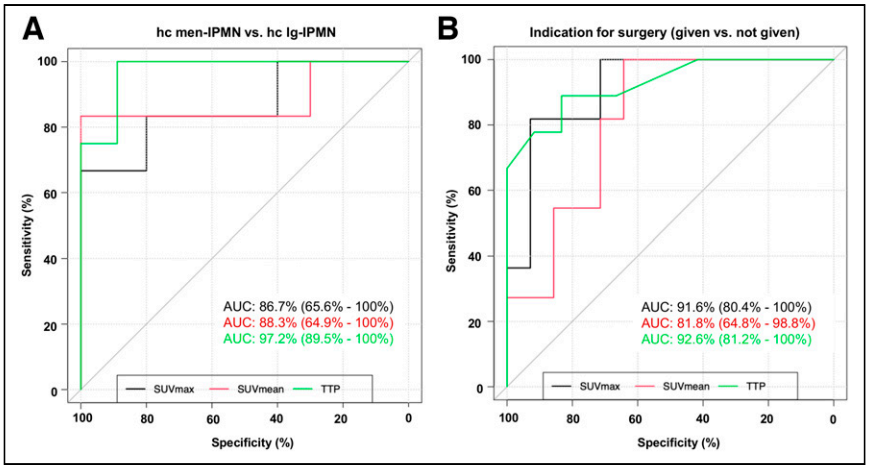

FIGURE 5. (A and B) Receiver-operating-characteristic (ROC) curves depicting sensitivity and specificity of quantitative static (SUV_{max} and SUV_{mean}) and dynamic (TTP) ^{68}Ga-FAPI-74 PET parameters for differentiation of histologically confirmed menacing IPMN and low-grade IPMN (A) and of lesions with and without indication for surgery (B). AUC = area under the curve.

and dilation of the branch duct by 16 mm. There were no symptoms of weight loss, abdominal pain, or pancreatitis. Laboratory results for CA 19-9, bilirubin, or inflammation were unremarkable; only lipase was slightly elevated (92 U/L, ULN 63 U/L). A diagnosis of mixed-type IPMN was made. ^{68}Ga-FAPI PET/CT showed a markedly increased SUV_{max} of 4.9. Via robotic assisted distal pancreatectomy, a mixed-type IPMN with high-grade dysplasia (pTis, N0) was successfully removed.

The patient with lg-IPMN was a 52-y-old woman who complained about abdominal pain. An abdominal ultrasound revealed a 60-mm cystic lesion in the pancreatic head without nodules or suspect perfusion on contrast-enhanced ultrasound. This lesion was confirmed on ceMRI and classified as a 60-mm side branch IPMN. The laboratory results were unremarkable. The medical history included a type 1 diabetes diagnosis with an onset at 2 y of age, complicated by neuropathy, retinopathy, and terminal nephropathy. In ^{68}Ga-FAPI PET/CT only a low accumulation was observed. As the size exceeded by far the guideline's limits, the cystic lesion was removed by laparoscopic robotic enucleation. Histologically a large branch duct IPMN with low-grade dysplasia was diagnosed.

DISCUSSION

Summary of Results

In this retrospective analysis of ^{68}Ga-FAPI-74 PET imaging in 25 patients with cystic pancreatic lesions, we observed significantly higher ^{68}Ga-FAPI-74 uptake measured as SUV_{max} and SUV_{mean} in men-IPMN than in lg-IPMN and other benign lesions. In dynamic ^{68}Ga-FAPI PET imaging, men-IPMN and lg-IPMN showed differential kinetic behavior, reflected by differences in TTP, K_1, and k_2 as well as K3 and k_4 values. The high diagnostic accuracy of static and dynamic ^{68}Ga-FAPI-74 PET for the differentiation of men-IPMN and lg-PMN was reflected by high AUC values in all ROC curves analyzed. These results suggest that ^{68}Ga-FAPI-74 PET is a promising new imaging technique for the clinical evaluation of pancreatic cystic lesions.

Static and Dynamic ^{68}Ga-FAPI-74 PET Imaging

We observed a high ^{68}Ga-FAPI-74 uptake in men-IPMN (with and without PDAC) and significantly lower ^{68}Ga-FAPI uptake in lg-IPMN, whereas healthy tissues had negligible background activity, leading to excellent contrast for suspicious lesions, similar to those shown by previous studies on ^{68}Ga-FAPI PET/CT in PDAC and other tumors (*19,20*). Next to static imaging results, we could

TABLE 2
Threshold and Specificity at Fixed Sensitivities of 90% and 80% for Differentiation Between Histologically Confirmed Low-Grade IPMN and Histologically Confirmed Menacing IPMN and Given Versus Not Given Indication for Surgery

Endpoint	Parameter	Threshold	Sensitivity (%)	95% CI	Specificity (%)	95% CI	TN	TP	FN	FP
lg/men	SUV_{max}	3.62	90.0	55.5–99.7	66.7	22.3–95.7	4	9	1	2
		4.85	80.0	44.4–97.5	83.3	35.9–99.6	5	8	2	1
lg/men	SUV_{mean}	2.07	90.0	55.5–99.7	83.3	35.9–99.6	5	9	1	1
		2.19	80.0	44.4–97.5	83.3	35.9–99.6	5	8	2	1
lg/men	TTP	135.00	88.9	51.8–99.7	100.0	39.8–100.0	4	8	1	0
		225.00	77.8	40.0–97.2	100.0	39.8–100.0	4	7	2	0
Surgery	SUV_{max}	3.62	90.9	58.7–99.8	71.4	41.9–91.6	10	10	1	4
		4.85	81.8	48.2–97.7	92.9	66.1–99.8	13	9	2	1
Surgery	SUV_{mean}	2.07	90.9	58.7–99.8	64.3	35.1–87.2	9	10	1	5
		2.19	81.8	48.2–97.7	71.4	41.9–91.6	10	9	2	4
Surgery	TTP	135	88.9	51.8–99.7	83.3	51.6–97.9	10	8	1	2
		225	77.8	40.0–97.2	91.7	61.5–99.8	11	7	2	1

FN = false negative; FP = false positive; lg/men = histologically confirmed low-grade IPMN vs. histologically confirmed menacing IPMN; TN = true negative; TP = true positive; TTP = time to peak. For some settings only approximate sensitivities could be selected due to sparsity of data.

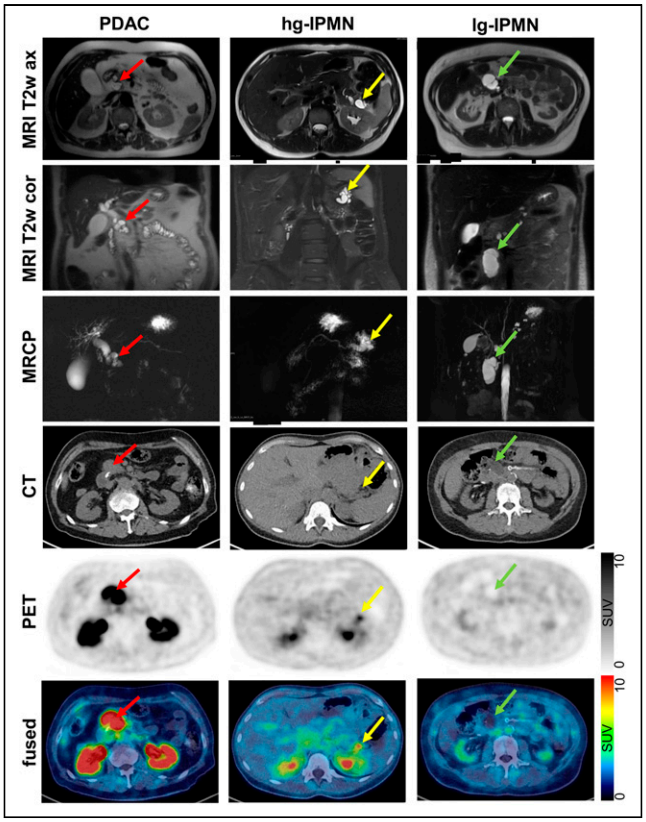

FIGURE 6. Representative axial and coronal T2-weighted MRI (MRI T2w ax and MRI T2w cor, respectively), MR cholangiopancreatography (MRCP), axial CT (CT ax), axial PET (PET ax), and fused images of a patient with hc hg-IPMN with progression into PDAC, a patient with hg-IPMN without PDAC, and patient with lg-IPMN. Red, yellow, and green arrows indicate pathologies.

demonstrate that dynamic imaging delivers additional diagnostic information and may improve the clinical classification of lg-IPMN and men-IPMN due to delayed binding and delayed washout of men-IPMN compared with lg-IPMN. These findings are in line with our previously published data on dynamic ^{68}Ga-FAPI PET imaging in patients with lung cancer and fibrosing interstitial lung diseases, for which we observed delayed washout of tumors compared with fibrotic lesions (*16*). Similarly, we could show in a previous project on ^{68}Ga-FAPI PET in PDAC that PDAC had a delayed washout compared with pancreatitis (*19*). Although the overall experience with dynamic behavior of ^{68}Ga-FAPI tracers is limited to few publications to date (*16,21,22*), delayed ^{68}Ga-FAPI washout appears to be sign of malignancy in this imaging method.

Risk Stratification of IPMN

To date, a compound of imaging, clinical, and laboratory criteria has been used to estimate the risk of malignant progression of IPMN. Most data exist on results of imaging techniques. Recent studies, mostly postoperative with a retrospective design, concluded that jaundice, a contrast-enhancing solid component or mural nodule, or a ≥ 10 mm main duct dilatation have a positive predictive value for malignancy of between 56% and 89% (*23–25*). A cyst size ≥ 30 mm without other clinical or radiologic risk factors has a low positive predictive value for malignant transformation of an IPMN ranging from 27% to 33% (*26–30*). Several studies regarding mostly surgically resected IPMN reported a wide risk range of 37%–91% for high-grade dysplasia or cancer for main duct dilatations of 5–9.9 mm (*31–33*). In patients after surgical resection of BD-IPMN, it was found that mural nodules ≥ 5 mm on EUS have a sensitivity of 73%–85% and specificity of 71%–100% for the presence of men-IPMN. Imaging detectability of mural nodes ≥ 10 mm on CT, MRI, ultrasound, and EUS were 64%, 68%, 89%, and 97%, respectively. Detectability of mural nodes ≥ 10 mm is excellent in abdominal and endoscopic ultrasound (*34–36*). In summary, main duct dilatation ≥ 10 mm and mural nodules on ultrasound examination are the most reliable factors. It must be considered that mural nodules are a rare condition. Next to morphologic imaging, PET/CT using ^{18}F-FDG has been applied in IPMN to detect malignancy based on increased glucose metabolism. For this approach, several older meta-analyses had calculated sensitivity and specificity rates of 80%–95% and 60%–95%, respectively (*37–40*), but more recent studies could not prove a benefit of ^{18}F-FDG PET/CT in IPMN (*41,42*). Given the low background activity of ^{68}Ga-FAPI radiotracers compared with ^{18}F-FDG in the pancreas and given the promising preliminary results of our study, one would expect that ^{68}Ga-FAPI PET may be superior to ^{18}F-FDG for the detection of malignancy in IPMN. On the basis of our data it appears that ^{68}Ga-FAPI-74 PET signal intensity and uptake kinetics offer high specificity and sensitivity for the detection of subtypes and may complement established predictors of malignancy.

Despite promising results, several limitations of our analysis must be considered. The major limitation of our study is the relatively small number of patients with IPMN included, especially with respect to dynamic imaging, which was performed in just 9 subjects. According to this, no definite conclusions should be drawn from our data, and further studies with more patients—including intraindividual comparisons of the diagnostic value for IPMN of ^{68}Ga-FAPI-74 PET and other imaging modalities such as CT, MRI, and ultrasound—are necessary to validate our findings. Another limitation arising from the sparsity of dynamic PET data is that our dataset does not allow a comparison between the discriminatory power of static alone versus dynamic alone versus combined static and dynamic imaging. An additional limitation is that not all patients included had undergone biopsy or surgery for definitive confirmation of their diagnoses. Although we considered the appearance of these lesions in MRI and ultrasound and the clinical course of the patients to gain valid clinical classifications, uncertainty remains for these cases, especially as our information available only reflects the status of the patients during a limited period of follow-up. Additionally, a certain selection bias may arise from the fact that all patients included into this analysis were referred by a highly specialized outpatient clinic. Thus, the dataset may not fully reflect the epidemiology of IPMN subtypes. However, a recently published study on the frequency of IPMN subtypes found a similar distribution of hg-IPMN and lg-IPMN (*10*). Taken together, our findings should be interpreted with caution and need confirmation in larger cohorts, optimally in prospective studies.

CONCLUSION

Static and dynamic ^{68}Ga-FAPI-74 PET/CT showed promising imaging properties for IPMN and predicted the grade of dysplasia of IPMN with high accuracy. We recommend further clinical evaluation of ^{68}Ga-FAPI-74 PET in combination with and comparison to MRI or EUS for the detection of malignant IPMN of the pancreas.

DISCLOSURE

This work was funded by the Federal Ministry of Education and Research (grant no. 13N 13341). Ulrike Heger, Clemens Kratochwil, and Frederik L. Giesel have filed a patent application for quinoline-based FAP-targeting agents for imaging and therapy in nuclear medicine. Ulrike Heger, Clemens Kratochwil, and Frederik L. Giesel also have shares of a consultancy group for iTheranostics. All procedures performed in studies involving human participants were in accordance with the ethical standards of the institutional or national research committee and with the 1964 Helsinki declaration and its later amendments or comparable ethical standards. This retrospective study was approved by the local institutional review board (study number S-115/2020). No other potential conflict of interest relevant to this article was reported.

KEY POINTS

QUESTION: Are static and dynamic ^{68}Ga-FAPI PET helpful for the discrimination of menacing (high-grade with and without progression into PDAC) and low-grade IPMN of the pancreas?

PERTINENT FINDINGS: Menacing IPMN with and without transformation into PDAC showed significantly higher ^{68}Ga-FAPI uptake than low-grade IPMN. Dynamic PET parameters (time to peak, K_1, k_2, K3, k_4) differed markedly between menacing and low-grade IPMN.

IMPLICATIONS FOR PATIENT CARE: ^{68}Ga-FAPI PET showed promising results with respect to the differentiation of menacing and low-grade IPMN and should be further evaluated in patients with IPMN or PDAC.

REFERENCES

1. Park W, Chawla A, O'Reilly EM. Pancreatic cancer: a review. *JAMA.* 2021;326:851–862.
2. Rezaee N, Barbon C, Zaki A, et al. Intraductal papillary mucinous neoplasm (IPMN) with high-grade dysplasia is a risk factor for the subsequent development of pancreatic ductal adenocarcinoma. *HPB (Oxford).* 2016;18:236–246.
3. Tanaka M, Fernandez-Del Castillo C, Kamisawa T, et al. Revisions of international consensus Fukuoka guidelines for the management of IPMN of the pancreas. *Pancreatology.* 2017;17:738–753.
4. European Study Group on Cystic Tumours of the Pancreas. European evidence-based guidelines on pancreatic cystic neoplasms. *Gut.* 2018;67:789–804.
5. Fritz S, Buchler MW, Werner J. Surgical therapy of intraductal papillary mucinous neoplasms of the pancreas [in German]. *Chirurg.* 2012;83:130–135.
6. Schnelldorfer T, Sarr MG, Nagorney DM, et al. Experience with 208 resections for intraductal papillary mucinous neoplasm of the pancreas. *Arch Surg.* 2008;143:639–646, discussion 646.
7. de Jong K, van Hooft JE, Nio CY, et al. Accuracy of preoperative workup in a prospective series of surgically resected cystic pancreatic lesions. *Scand J Gastroenterol.* 2012;47:1056–1063.
8. Morris-Stiff G, Lentz G, Chalikonda S, et al. Pancreatic cyst aspiration analysis for cystic neoplasms: mucin or carcinoembryonic antigen—which is better? *Surgery.* 2010;148:638–644, discussion 644–635.
9. Heckler M, Brieger L, Heger U, et al. Predictive performance of factors associated with malignancy in intraductal papillary mucinous neoplasia of the pancreas. *BJS Open.* 2018;2:13–24.
10. Tjaden C, Sandini M, Mihaljevic AL, et al. Risk of the watch-and-wait concept in surgical treatment of intraductal papillary mucinous neoplasm. *JAMA Surg.* 2021;156:818–825.
11. von Ahrens D, Bhagat TD, Nagrath D, Maitra A, Verma A. The role of stromal cancer-associated fibroblasts in pancreatic cancer. *J Hematol Oncol.* 2017;10:76.
12. Hanahan D, Weinberg RA. Hallmarks of cancer: the next generation. *Cell.* 2011;144:646–674.
13. Lindner T, Loktev A, Altmann A, et al. Development of quinoline-based theranostic ligands for the targeting of fibroblast activation protein. *J Nucl Med.* 2018;59:1415–1422.
14. Lindner T, Altmann A, Giesel F, et al. ^{18}F-labeled tracers targeting fibroblast activation protein. *EJNMMI Radiopharm Chem.* 2021;6:26.
15. Loktev A, Lindner T, Mier W, et al. A tumor-imaging method targeting cancer-associated fibroblasts. *J Nucl Med.* 2018;59:1423–1429.
16. Röhrich M, Leitz D, Glatting FM, et al. Fibroblast activation protein-specific PET/CT imaging in fibrotic interstitial lung diseases and lung cancer: a translational exploratory study. *J Nucl Med.* 2022;63:127–133.
17. DeLong ER, DeLong DM, Clarke-Pearson DL. Comparing the areas under two or more correlated receiver operating characteristic curves: a nonparametric approach. *Biometrics.* 1988;44:837–845.
18. Robin X, Turck N, Hainard A, et al. pROC: an open-source package for R and S+ to analyze and compare ROC curves. *BMC Bioinformatics.* 2011;12:77.
19. Röhrich M, Naumann P, Giesel FL, et al. Impact of $^{(68)}$Ga-FAPI-PET/CT imaging on the therapeutic management of primary and recurrent pancreatic ductal adenocarcinomas. *J Nucl Med.* 2021;62:779–786.
20. Kratochwil C, Flechsig P, Lindner T, et al. ^{68}Ga-FAPI PET/CT: tracer uptake in 28 different kinds of cancer. *J Nucl Med.* 2019;60:801–805.
21. Wang S, Zhou X, Xu X, et al. Dynamic PET/CT imaging of ^{68}Ga-FAPI-04 in Chinese subjects. *Front Oncol.* 2021;11:651005.
22. Geist BK, Xing H, Wang J, et al. A methodological investigation of healthy tissue, hepatocellular carcinoma, and other lesions with dynamic ^{68}Ga-FAPI-04 PET/CT imaging. *EJNMMI Phys.* 2021;8:8.
23. Fritz S, Klauss M, Bergmann F, et al. Pancreatic main-duct involvement in branch-duct IPMNs: an underestimated risk. *Ann Surg.* 2014;260:848–855, discussion 855–846.
24. Roch AM, Ceppa EP, DeWitt JM, et al. International consensus guidelines parameters for the prediction of malignancy in intraductal papillary mucinous neoplasm are not properly weighted and are not cumulative. *HPB (Oxford).* 2014;16:929–935.
25. Goh BK, Thng CH, Tan DM, et al. Evaluation of the Sendai and 2012 international consensus guidelines based on cross-sectional imaging findings performed for the initial triage of mucinous cystic lesions of the pancreas: a single institution experience with 114 surgically treated patients. *Am J Surg.* 2014;208:202–209.
26. Sahora K, Mino-Kenudson M, Brugge W, et al. Branch duct intraductal papillary mucinous neoplasms: does cyst size change the tip of the scale? A critical analysis of the revised international consensus guidelines in a large single-institutional series. *Ann Surg.* 2013;258:466–475.
27. Aso T, Ohtsuka T, Matsunaga T, et al. "High-risk stigmata" of the 2012 international consensus guidelines correlate with the malignant grade of branch duct intraductal papillary mucinous neoplasms of the pancreas. *Pancreas.* 2014;43:1239–1243.
28. Nguyen AH, Toste PA, Farrell JJ, et al. Current recommendations for surveillance and surgery of intraductal papillary mucinous neoplasms may overlook some patients with cancer. *J Gastrointest Surg.* 2015;19:258–265.
29. Dortch JD, Stauffer JA, Asbun HJ. Pancreatic resection for side-branch intraductal papillary mucinous neoplasm (SB-IPMN): a contemporary single-institution experience. *J Gastrointest Surg.* 2015;19:1603–1609.
30. Robles EP, Maire F, Cros J, et al. Accuracy of 2012 international consensus guidelines for the prediction of malignancy of branch-duct intraductal papillary mucinous neoplasms of the pancreas. *United European Gastroenterol J.* 2016;4:580–586.
31. Seo N, Byun JH, Kim JH, et al. Validation of the 2012 international consensus guidelines using computed tomography and magnetic resonance imaging: branch duct and main duct intraductal papillary mucinous neoplasms of the pancreas. *Ann Surg.* 2016;263:557–564.
32. Hackert T, Fritz S, Klauss M, et al. Main-duct intraductal papillary mucinous neoplasm: high cancer risk in duct diameter of 5 to 9 mm. *Ann Surg.* 2015;262:875–880, discussion 880–871.
33. Abdeljawad K, Vemulapalli KC, Schmidt CM, et al. Prevalence of malignancy in patients with pure main duct intraductal papillary mucinous neoplasms. *Gastrointest Endosc.* 2014;79:623–629.
34. Kawada N, Uehara H, Nagata S, Tsuchishima M, Tsutsumi M, Tomita Y. Mural nodule of 10 mm or larger as predictor of malignancy for intraductal papillary mucinous neoplasm of the pancreas: pathological and radiological evaluations. *Pancreatology.* 2016;16:441–448.
35. Kobayashi N, Sugimori K, Shimamura T, et al. Endoscopic ultrasonographic findings predict the risk of carcinoma in branch duct intraductal papillary mucinous neoplasms of the pancreas. *Pancreatology.* 2012;12:141–145.
36. Shimizu Y, Yamaue H, Maguchi H, et al. Predictors of malignancy in intraductal papillary mucinous neoplasm of the pancreas: analysis of 310 pancreatic resection patients at multiple high-volume centers. *Pancreas.* 2013;42:883–888.

37. Best LM, Rawji V, Pereira SP, Davidson BR, Gurusamy KS. Imaging modalities for characterising focal pancreatic lesions. *Cochrane Database Syst Rev.* 2017;4: CD010213.
38. Xu MM, Yin S, Siddiqui AA, et al. Comparison of the diagnostic accuracy of three current guidelines for the evaluation of asymptomatic pancreatic cystic neoplasms. *Medicine (Baltimore)*. 2017;96:e7900.
39. Sultana A, Jackson R, Tim G, et al. What is the best way to identify malignant transformation within pancreatic IPMN: a systematic review and meta-analyses. *Clin Transl Gastroenterol.* 2015;6:e130.
40. Bertagna F, Treglia G, Baiocchi GL, Giubbini R. F18-FDG-PET/CT for evaluation of intraductal papillary mucinous neoplasms (IPMN): a review of the literature. *Jpn J Radiol*. 2013;31:229–236.
41. Regenet N, Sauvanet A, Muscari F, et al. The value of ^{18}F-FDG positron emission tomography to differentiate benign from malignant intraductal papillary mucinous neoplasms: a prospective multicenter study. *J Visc Surg.* 2020;157:387–394.
42. Liu H, Cui Y, Shao J, Shao Z, Su F, Li Y. The diagnostic role of CT, MRI/MRCP, PET/CT, EUS and DWI in the differentiation of benign and malignant IPMN: A meta-analysis. *Clin Imaging.* 2021;72:183–193.